A New Formulation for Optimal Tuning of Fast Frequency Support in Multi-Energy Systems

Georgios Giannakopoulos, Arcadio Perilla
Intelligent Electrical Power Grids
Delft University of Technology
Delft, The Netherlands
[G.Giannakopoulos, A.Perilla]@tudelft.nl

Jose Rueda Torres, Peter Palensky
Intelligent Electrical Power Grids
Delft University of Technology
Delft, The Netherlands
[j.l.ruedatorres, P.Palensky]@tudelft.nl

Abstract*—Power electronic dominated power systems formed nowadays are characterized by fast and frequent dynamics, limited short circuit support, low inertia conditions and lack of inertial support. Under these conditions, coping with active power imbalances in a power system may becomes a significant challenge for transmission system operators (TSOs) that may experience extensive frequency deviations and steep rates of change of frequency (RoCofs). To deal with the frequency stability issues encountered, power electronic interfaced (PEI) units can rapidly respond to provide fast frequency support (FFS) taking advantage of their controllability levels and their rapid response to setpoint changes. FFS may depend on the active power gradient (APG) control strategy that determines the required amount of active power, and the rate the power injection takes place. However, when multiple elements try to regulate simultaneously the frequency adverse control actions such as insufficient or over frequency regulation may be encountered. To solve this issue, this paper proposes a formulation for the optimal and coordinative tuning of the APG controllers of PEI elements installed in a multi-area, multi-energy hybrid HVDC/HVAC power system with modular multilevel converter (MMC) HVDC links and proton exchange membrane (PEM) electrolyzers. This formulation focuses on creating an artificially coupled frequency response for an electromagnetically decoupled multi-area system taking advantage of the available active power reserves and the inertia levels of each area. In that way, an active power imbalance can be optimally shared among the interconnected areas leading to effectively improved frequency response for the affected and supporting areas. The proposed formulation is solved using the mean variance mapping optimization (MVMO) algorithm after a series of RMS simulations is performed in DIgSILENT PowerFactory 2021.

Keywords—Active power gradient, fast active power-frequency support, frequency controllers tuning, mean variance mapping optimization, MMC-HVDC links, PEM electrolyzers

I. Introduction

Power systems nowadays are characterized by an increasing number of power electronic interfaces (PEIs) [1][2]. Power electronics (PEs) are met at various system points such as for the renewable energy sources' (RES') interconnection to the grid, to enable HVDC transmission via VSC-based HVDC links, in distributed energy sources (DERs) interconnection, in energy storage systems (ESSs), in hydrogen-based units and in critical demand units [1][3]. Hence, the form and the structure of modern power systems is altered, leading also to various impacts on its dynamic response [4]. In fact, such systems face fast and frequent dynamics, reduced short circuit contribution, low inertia conditions, lack of natural inertial response and lack of load-frequency regulation [4][5]. As a result, preserving the frequency within acceptable operating state limits becomes one of the main challenges for transmission system operators (TSOs) as large frequency deviations and steep rates of change of frequency (RoCofs) may be encountered for common active power imbalances [4][6].

To solve this issue, PEIs of newly introduced elements may be enhanced with frequency control systems to provide fast frequency support (FFS) to the grid when necessary, taking advantage of the control capabilities of PEs [7]. FFS may be provided by various elements such as wind turbines (WTs)[8], solar-photovoltaic systems (PVs)[9], HVDC links [10] and hydrogen-based units [11]. Among the different techniques, the active power gradient control strategy presented in [12] has shown high potential for FFS through the control of two parameters, the amount of active power (ΔP) and the rate (APG) this power is provided to the grid following the disturbance. This strategy may be easily applied to PE converters of various elements installed in the grid aiming at cooperative FFS in case of an active power imbalance. This task, however, may be challenging if an optimal tuning of the parameters of the frequency controllers of the elements providing FFS is not achieved [12][13]. Research conducted in [12] has proven the difficulty in finding the optimal tuning parameters in case of a point-to-point VSC-based HVDC link providing FFS in case of two-area system with similar inertia characteristics. The situation gets worse when more elements with different response characteristics participate in the regulation as has been observed in [13]. To solve this issue, current state-of-art research aims to find an optimal tuning method of the parameters of frequency controllers attached to various PEI elements with the provision of FFS to the grid. In [13] and [14] different problem formulations have been proposed to tune the parameters of frequency controllers attached to HVDC links and proton exchange membrane (PEM) electrolyzers to improve the frequency stability margin of two-area, low-inertia multi-energy systems. Although these formulations may achieve significantly improved responses against commonly occurred active power imbalances, the determination of a coordinative tuning strategy in more complex multi-area systems with an increased number of FFS elements constitutes an open research gap.

This paper aims to shed light on this research gap by proposing a new formulation to achieve an optimal and coordinative tuning of the frequency controllers attached to MMC-based HVDC links and PEM electrolyzers installed at various points of a multi-area, multi-energy hybrid HVDC/HVAC power system following the occurrence of a significant active power imbalance. This formulation aims to improve the frequency stability margin of the system by sharing the imbalance among the available areas taking advantage of their active power reserve characteristics and their inertia levels. In fact, it tries to achieve similar frequency responses to all the interconnected areas in order not only to

2022 IEEE Power & Energy Society General Meeting (PESGM) | 978-1-6654-0823-3/22/$31.00 ©2022 IEEE | DOI: 10.1109/PESGM48719.2022.9916836

978-1-6654-0823-3/22/$31.00 ©2022 IEEE

improve the frequency response of the affected area, but also to minimize the impact on the supporting areas at the maximum extend. To solve this optimization problem, a series of RMS simulations is performed in DIgSILENT PowerFactory 2021(DPF). The frequency responses obtained, act as inputs to the optimization problem developed under the proposed formulation in Python 3.8. Finally, the optimization problem is solved with the aid of the mean variance mapping optimization (MVMO) algorithm that has achieved results of high quality in short number of iterations in power system problems with high computational burden [22].

The structure of the paper is as follows: Section II gives an overview of the test system, the modified PST 16 power system considered in this study. In Section III, the proposed problem formulation is presented in detail. In Section IV the MVMO algorithm is briefly explained. In Section V, the obtained numerical results are discussed and finally in Section VI the conclusions of the current study and proposals for future work are provided.

II. The Modified PST 16 Benchmark System

To test the tuning methodology proposed in this paper and perform the RMS simulations of interest, a modified version of the PST 16 power system presented in [15] has been utilized. In the modified system shown in Fig. 1, three MMC-based HVDC links have replaced the weak HVAC tie-lines among the areas of the original system. Also, 30% of the original load demand of each area has been replaced by eleven PEM electrolyzers according to the expected hydrogen demand scenario analyzed in [16]. Electrolyzers are installed at various points to examine the importance of location of installation with respect to the disturbance. In that way, a multi-area, multi-energy HVDC/HVAC power system can be represented. Further details about the modified PST 16 system can be found in [27].

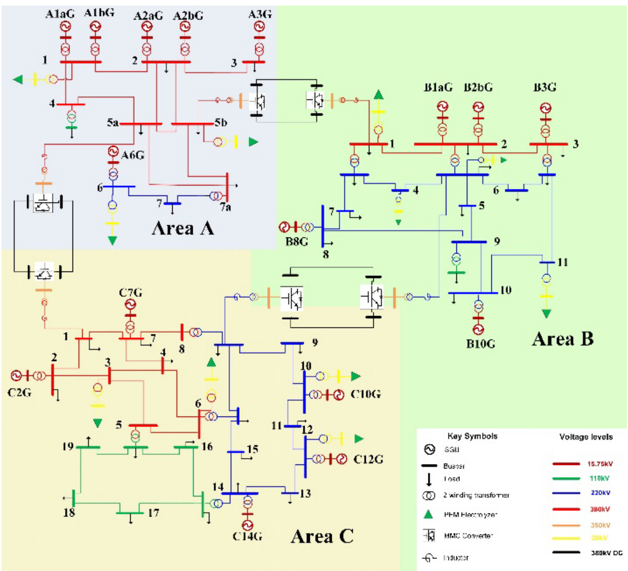

Fig. 1. The Modified PST 16 benchmark system.

For the modelling of the MMC-HVDC links in DPF, a model provided by DIgSILENT presented in [17] has been considered developed under the guidelines in [18]. It consists of two converter stations controlled with the aid of the current-vector control strategy presented in [19]. The converter stations are connected on the DC side in a bipolar configuration and on the AC side via power transformers to the local grid. During steady state, the necessary active and reactive power setpoints have been provided to the HVDC links to facilitate the normal power flows of the original system. The inverter stations control the power output with respect to active and reactive power setpoints and the rectifiers according to DC voltage and reactive power setpoints to maintain the active power balance across the link. Furthermore, to enable FFS from the HVDC links, the P/Vdc controller of each link has been modified according to Fig. 2 with the APG control loop to control the amount of power (ΔP) and the injection rate of the active power (APG) in case of a sensed frequency deviation. The parameter selection is done according to the solution of the optimization problem under the proposed formulation according to the frequency responses of each area as it will be explained in Section III. The HVDC links alter their power flows for FFS once per simulation, 0.3s following the disturbance to consider an activation delay.

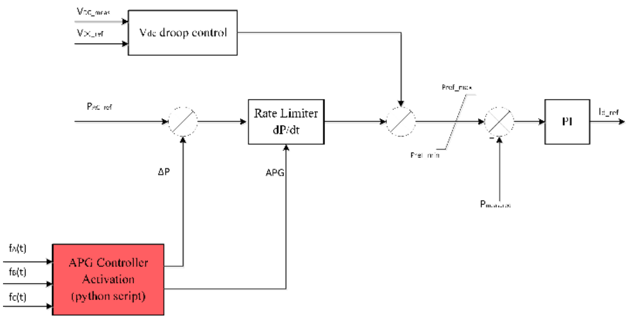

Fig. 2. Modified P/Vdc controller of MMC-HVDC links.

PEM electrolyzers have been modelled in this study as electromagnetically decoupled general loads interconnected via power transformers to the local grid according to [20]. The consumption of the electrolyzers is dynamically controlled proportionally to sensed frequency deviations when they are activated for FFS following the control structure shown in Fig. 5. The frequency controllers are tuned in terms of the available bid and the ramp rate the injection takes place considering the APG control block shown in Fig 3. This block determines the available bid and the ramp rate according to the solution of the optimization problem under the proposed formulation as explained in Section III. The latter representation of the PEM electrolyzers is a simple yet accurate representation for power system stability studies as explained in [20] considering the main parameter of interest, the ramp rate of the consumption of the electrolyzers.

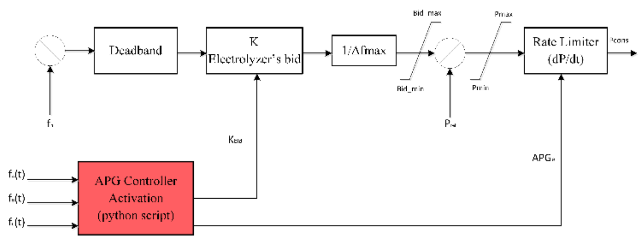

Fig. 3. Dynamic frequency controller of PEM electrolyzers.

III. Problem Formulation

When a system consists of multiple areas electromagnetically decoupled via MMC-based HVDC links, each area is characterized by its own frequency. When an active power imbalance occurs in one of the areas, the imbalance is reflected on the frequency of the latter area [21].

978-1-6654-0823-3/22/$31.00 ©2022 IEEE

The frequency in other areas remains constant at its nominal value, unless the HVDC links alter their power flows with the provision of FFS to the affected area. In the latter case, the frequency in the supporting areas deviates from 50Hz, according to the changes in the power flows among the areas.

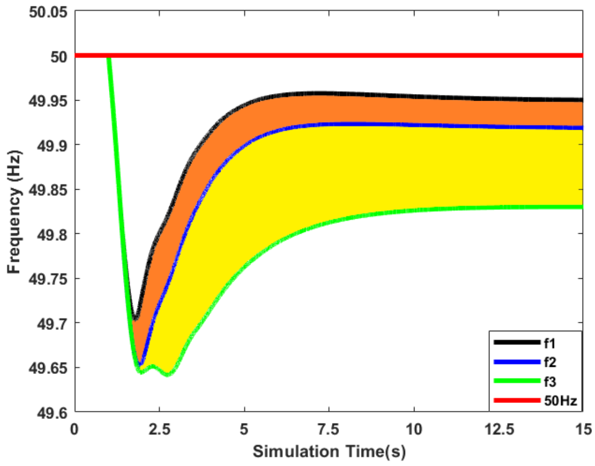

Fig. 4. Problem Formulation graphical representation.

According to this representation, in the three-area system of interest, the proposed problem formulation (OF) aims to minimize the graphical area among each pair of the frequency responses of the areas participating in the frequency regulation as it can be observed in Fig. 4. In that way, it aims to share the active power imbalance among the areas according to their active power reserve and inertia characteristics, and thus, improve the frequency response of the affected area with the minimum impact on the supporting areas. In fact, it tries to create an artificially coupled frequency response in a decoupled multi-area system and thus obtain the best frequency response for the whole system by optimally distributing the imbalance across the available reserves of each area. Mathematically, this problem formulation can be represented with by (1)-(7).

$$\text{Minimize: } OF(\mathbf{x})=\int_0^{\tau}[|f_A(\mathbf{x},t)-f_B(\mathbf{x},t)| + |f_B(\mathbf{x},t)-f_C(\mathbf{x},t)|+ |f_A(x,t)-f_C(x,t)|dt \quad (1)$$

$$\text{subjected to: } \mathbf{x}_{min}\leq\mathbf{x}\leq\mathbf{x}_{max} \quad (2)$$

Where $f_k(\mathbf{x},t)$ is the instantaneously measured frequency in the k-th area at t instant when the candidate **x** has been applied. The optimization vector **x** contains two variables for each of the FFS elements that participate in the frequency regulation. Since three MMC-HVDC links and eleven electrolyzers have been installed in the modified PST 16 system, 28 optimization variables constitute **x**. For the HVDC links the first parameter reflects the ramp rate of the active power (APG) and the second one the change in the active power flow of the corresponding link (ΔP). For the PEM electrolyzers, the first parameter reflects the bid size of the electrolyzer (Bid_e) and the second parameter the rate of change of the electrolyzer's consumption (APG_e). The optimization vector **x** can be observed in (3). Finally, each of the optimization variables is bounded according to the technical limitations of each unit. For the HVDC links, the new setpoint may not overcome the rated capacity of the link in both directions [13][14] and the ramp rate should not exceed the maximum rate the link may handle [23]. Similarly, for the PEM electrolyzers the available bid may not overcome 70% of its rated capacity and the ramp rate is considered that should not overcome 0.5pu/s as explained in [20],[24] and [25]. The boundary condition of the considered optimization variables can be observed in (4)-(7).

$$\mathbf{x}=\begin{bmatrix}\Delta P_{HVDC_1},APG_{HVDC_1},\ldots,\Delta P_{HVDC_i},APG_{HVDC_i},K_{ebid_1}, \\ APG_{e_1},\ldots,K_{ebid_j},APG_{e_j}\end{bmatrix} \quad (3)$$

$$P_{refi}+\Delta P_i\leq|P_{rated_i}| \quad (4)$$

$$0\frac{GW}{min}\leq APGi\leq 60\frac{GW}{min} \quad (5)$$

$$0\leq K_{bid_w}\leq 0.7P_{elec_{rate_w}} \quad (6)$$

$$0\leq APG_{e_w}\leq 0.5\ P_{elec_{rated_w}}\ \frac{MW}{s} \quad (7)$$

IV. The Mean Variance Optimization Algorithm

To solve the optimization problem developed, a powerful metaheuristic algorithm, the mean variance optimization (MVMO) algorithm has been utilized. This algorithm has shown great potential in solving computationally expensive problems in power system applications [22]. The complete MVMO flowchart can be observed in Fig.5. The MVMO calculates initially a random initial vector within the available research space defined by the boundary conditions considered for each variable. Then it applies the selected parameters in the corresponding element of the system in DPF and performs an RMS simulation to obtain the frequency responses of interest. The latter ones are utilized to perform the fitness evaluation and calculate the value of the OF. The same process is followed for a number of predefined fitness evaluations which in this study has been considered to be equal to 100, acting as a termination criterion of the algorithm. Throughout these iterations, the MVMO is able to generate offspring candidate solution vectors according to the optimization variables of the best achieved parent solution so far and with respect to the evolution guidelines provided by a mapping function for each variable having as inputs statistical data such as the mean and the variance of each optimization variable. For this reason, the best parent solutions achieved and statistical data for each variable are stored in an archive of a predefined size. Finally, when the termination criterion has been fulfilled the solution vector contains the variables that achieved the minimum OF value and thus the best frequency response for the system within the number of fitness evaluations. This algorithm, operates in a normalized range [0,1] for each variable and thus, it avoids penalties or corrections at a later stage. Further details about the MVMO algorithm can be found in [22].

V. Simulation Study and Numerical Results

To evaluate the effectiveness of the proposed formulation for the tuning of the frequency controllers of the HVDC links and PEM electrolyzers, a significant commonly occurred active power imbalance in the modified PST 16 system has been considered. This event comprises of the loss of the largest generating unit (SGU A1a) in the area with the lowest inertia conditions, area A. This event takes place at the first second of the simulation and following the disturbance all the PEI elements installed in all the areas are triggered to provide FFS.

978-1-6654-0823-3/22/$31.00 ©2022 IEEE

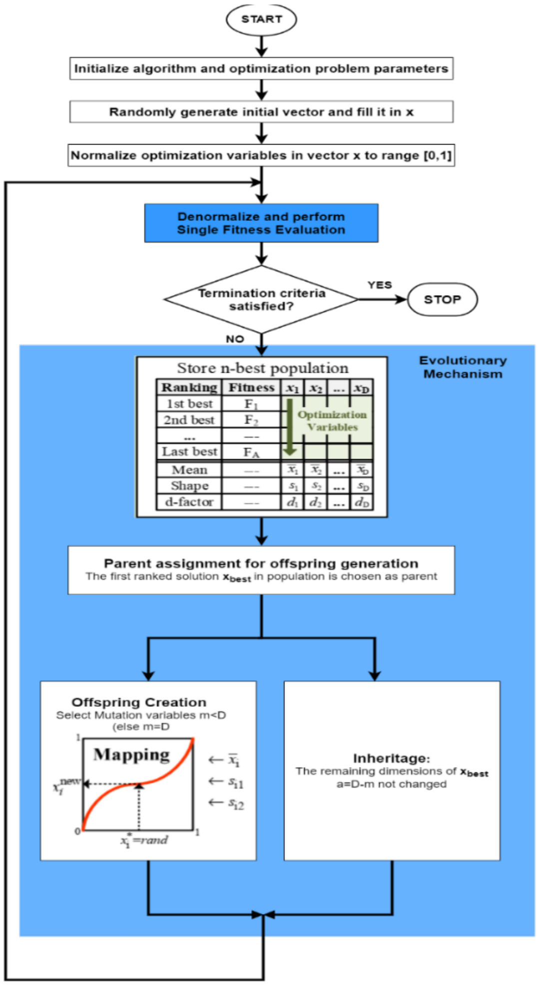

Fig. 5. The MVMO algorithm process.

In case no FFS is provided by any PEI element, the SGUs in the affected area are the only elements that can shoulder the frequency control. In this scenario, the frequency in area A drops rapidly at a rate equal to -0.51Hz/s to 48.8Hz and then starts to recover before finally stabilizing after almost 15s at 49.55Hz. The frequency in areas B,C remains unaffected as the HVDC links isolate the affected area from the rest of the system and no modifications are applied to their power flows. The latter response can be observed in Fig. 6 in dashed line. As it is clear, the frequency response in the affected area violates the acceptable limits set by TSOs in [26] and thus FFS from PEI units is required.

If now, PEI elements are activated to provide FFS, the proposed problem formulation can be used to tune the parameters of their controllers. After the termination criterion has been fulfilled, the solution vector **x** has the form shown in (8) and the corresponding frequency response of the system may be observed in Fig. 6 in solid style. As it is clear, the frequency in the affected area significantly improves when the imbalance is shared among the available areas. The initial RoCof shrinks to -0.30Hz/s from -0.51Hz/s, due to the rapid response of the PEM electrolyzers in the affected area. Then, the frequency in area A drops to 49.76Hz and stabilizes at 49.93Hz within 5s. The frequency in areas B and C drops to 49.92Hz and 49.93Hz, respectively before stabilizing at 49.93Hz and 49.94Hz, respectively. This confirms that the goal of the proposed formulation to minimize the frequency drop in the affected with the minimum impact on the supporting areas can be achieved if proper tuning is performed. In that way, the formulation tries to create similar frequency responses for all the interconnected areas utilizing the available reserves and thus achieves frequency responses within the acceptable operating limits set by TSOs in [26].

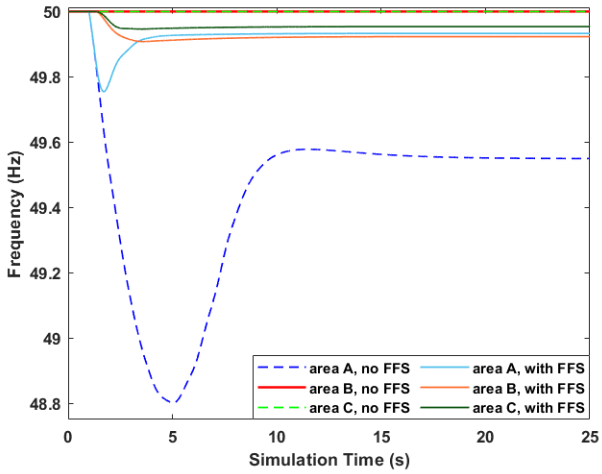

Fig. 6. Areas' frequency response without and with FFS.

$$\mathbf{x}=[932,-185,796,-377,412,-188.9,95.4,67.5,38.7,72.2,21.4,62.3,242,121,85.6,29.2,186,36.7,12.1,16.4,166,74.5,32.9,24.7,45.9,94.5,118,53.5] \quad (8)$$

Also, it is evident from (8), that the role of the electrolyzers is also significantly important for the FFS. In fact, PEM electrolyzers in area A, are activated to provide rapid support following the imbalance and arrest the initial drop before the activation of the HVDC links. After 0.3s, the HVDC links AB and AC alter their power flows and reduce the exports to areas B and C to support the affected area, whereas HVDC link BC changes its flow direction to balance the impact on areas B and C. In that way, the formulation achieves an optimal share among the areas according to their active power reserve and inertia characteristics. PEM electrolyzers in areas B and C are also activated for FFS to minimize the impact on the supporting areas and lead to similar post disturbance frequency responses. As a result, the formulation tries to achieve a coupled frequency response for an electromagnetically decoupled multi-area system.

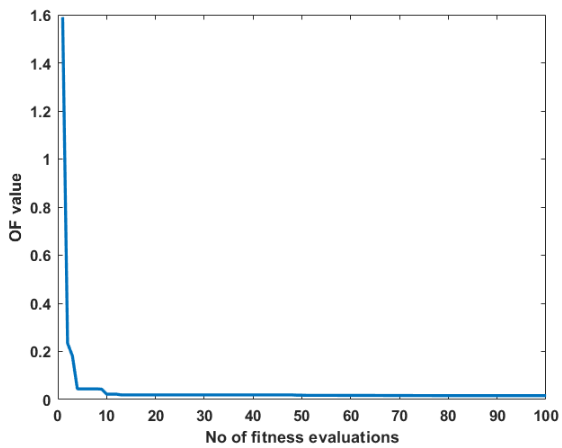

Fig. 7. Convergence of the Objective Function value.

Finally, considering the performance of the algorithm, Fig.7 can be observed. As it is clear, the MVMO can effectively reduce the value of the proposed OF within a very short number of iterations significantly reducing the computational burden and achieving results of great quality in terms of frequency response.

VI. Conclusions

In this paper, a new formulation for the optimal and coordinative tuning of the parameters of the frequency controllers of PEI elements with the provision of FFS in a multi-area, multi-energy hybrid HVDC/HVAC power system has been proposed and analyzed. This formulation aims at creating an artificially coupled frequency response for an electromagnetically decoupled multi-area system. In that way, an active power imbalance can be optimally shared across the areas according to their reserve and inertia characteristics and achieve significantly improved frequency response for the affected area with the minimum impact on the supporting areas. Also, the formulation can preserve the frequency in all areas within the acceptable limits set by TSOs considering the RoCof, the nadir and its post disturbance steady state deviation. The solution of the optimization problem achieved results of high quality within a short number of fitness evaluations when the MVMO algorithm has been used. In future research, the same formulation will be applied in a larger scale multi-energy system combining different FFS sources and considering different frequency control techniques. Moreover, different optimization algorithms and initial solutions will be considered to evaluate the most effective tuning strategy for large scale multi-area multi-energy systems.

References

[1] A. Halley, N. Martins, P. Gomes, D. Jacobson, W. Sattinger, Y. Fang, L. Haarla, Z. Emin, M. Val Escudero, S. Almeida De Graaff, V. Sewdien and A. Bose: “Effects of increasing power electronics-based technology on power system stability: Performance and operations”, CIGRE Science & Engineering, vol. 11, pp. 5-17, June 2018.

[2] A. Khan, M. Hosseinzadehtaher, M. B. Shadmand, S. Bayhan and H. Abu-Rub, “ On the Stability of the Power Electronics-Dominated Grid: A New Energy Paradigm,” in IEEE Industrial Electronics Magazine, vol.14,no.4,pp.65-78, Dec. 2020, doi: 10.1109/MIE.2020.3002523.

[3] Yuan, X., Hu, J. & Cheng, S.”Multi-time scale dynamics in power electronics-dominated power systems,” Front. Mech. Eng. 12, 303–311 (2017). https://doi.org/10.1007/s11465-017-0428-z.

[4] N. Hatziargyriou, J. V. Milanović, C. Rahmann, V. Ajjarapu, C. Cañizares, I. Erlich, D. Hill, I. Hiskens, I. Kamwa, B. Pal, P. Pourbeik, J. J. Sanchez- Gasca, A. Stanković, T. Van Cutsem, V. Vittal and C. Vournas: “Definition and Classification of Power System Stability – Revised and Extended”, IEEE Transactions on Power Systems, December 2020.

[5] L. Meegahapola, A. Sguarezi, J.S. Bryant, M. Gu, D. E. R.Conde R. B. A. Cunha. “Power System Stability with Power-Electronic Converter Interfaced Renewable Power Generation: Present Issues and Future Trends”,Energies 2020, 13,3441. https://doi.org/10.3390/en13133441.

[6] V.N. Sewdien, R. Chatterjee, M. Val Escudero, and J. Van Putten,“System Operational Challenges from the Energy Transition,” CIGRE Science & Engineering, vol.17, pp. 5-19, Feb. 2020.

[7] P Maibach, A. Hernandez, J. Peiro, C. Smith, V. Sewdien and J. van Putten, “ Capabilities of Power Electronic Devices in Enabling the Energy Transition and Mitigating System Operational Challenges,” CIGRE Science & Engineering, vol.20, pp. 125-136, Feb. 2021.

[8] E. Rakhshani, A. Perilla, J. L. R. Torres, F. M. Gonzalez-Longatt, T. B. Soeiro and M. A. M. M. Van Der Meijden, "FAPI Controller for Frequency Support in Low-Inertia Power Systems," in IEEE Open Access Journal of Power and Energy, vol. 7, pp. 276-286, 2020, doi: 10.1109/OAJPE.2020.3010224.

[9] Crăciun, B., Kerekes T., Séra D., Teodorescu R., and Annakkage U., Power ramp limitation capabilities of large PV power plants with active power reserves. IEEE Transactions on Sustainable Energy, vol. 8, no. 2, pp. 573–581, 2017.

[10] Karaolanis, A., Perilla A., Rueda, J.L., van der Meijden M., and Alefragkis A., Generic model of a VSC-based HVDC link for RMS simulations in PSS/E. IFAC-PapersOnLine, vol. 51, no. 28, pp. 303 – 308, 10th IFAC Symposium on Control of Power and Energy Systems CPES, 2018.

[11] N. Veerakumar, Z. Ahmad, M. Ebrahim Adabi, J. L. Rueda Torres, P. Palensky, M.A.M.M. van der Meijden, F. Gonzalez-Longatt, “Fast Active Power - Frequency Support Methods in Large Scale Electrolyzers for Multi-Energy Systems”, in 2020 IEEE PES Innovative Smart Grid Technologies Europe (ISGT-Europe), The Hague, The Netherlands, October 2020.

[12] A.D. Perilla Guerra, J. L. Rueda Torres, A.A. van der Meer, M.A.M.M. van den Meijden and A. Alefragkis, “Influence of Active Power Gradient Control of an MMC-HVDC Link on Long-Term Frequency Stability”, in 2017 IEEE Power & Energy Society General Meeting, Chicago, IL, USA 2017.

[13] A.D. Perilla Guerra, D. Gusain, J.L. Rueda Torres, P. Palensky, M.A.M.M. van der Meijden, F. Gonzalez-Longatt, “Optimal Tuning of Active Power Control for Frequency Support in Multi-Energy Systems”, in 2020 IEEE PES Innovative Smart Grid Technologies Europe (ISGT-Europe), The Hague, The Netherlands, October 2020.

[14] J.L. Rueda Torres, A.D. Perilla Guerra, E. Rakhshani, P. Palensky, M.A.M.M. van der Meijden and A. Alefragkis, “MVMO-based Tuning of Active Power Gradient Control of VSC-HVDC Links for Frequency Support”, in 2019 2nd International Conference on Smart Grid and Renewable Energy(SGRE), Doha, Qatar, 2019.

[15] F. M. Gonzalez-Longatt and J. L. Rueda Torres, “PowerFactory Applications for Power System Analysis”, Springer, Delft, The Netherlands, 2014.

[16] Hydrogen Council, “ Hydrogen Scaling up – A Sustainable Pathway for the Global Energy Transition”, Hydrogen Council Tech. Rep., Nov. 2017.

[17] DIgSILENT GmbH, “PowerFactory Seminar HVDC and Facts”, DIgSILENT GmbH, Tech. Rep., June 2018, Gomaringen, Germany.

[18] CIGRE Working Group B4.57, “Guide for the Development of Models for HVDC Converters in a HVDC Grid”, CIGRE, Tech. Rep., December 2014.

[19] N. T. Trinh, M. Zeller, K. Wuerflinger, and I. Erlich, “Generic Model of MMC-VSC-HVDC for Interaction Study With AC Power System,” IEEE Transactions on Power Systems, vol.31, no.1, pp.27-34, Jan. 2016.

[20] “Stability Analysis of an International Electricity System Connected to Regional Local Sustainable Gas Systems”, TSO 2020 Activity 2 Final Report, 2019.

[21] P. Kundur, “ Power System Stability and Control”, McGraw-Hill Professional, 1st Edition, 1994.

[22] J. L. Rueda Torres and I. Erlich, “ Hybrid Single Parent-Offspring MVMO for Solving CEC2018 Computationally Expensive Problems”, 2018 IEEE World Congress on Computational Intelligence, pp. 1-8, Rio de Janeiro Brazil, July 2018.

[23] Wang, W., Beddard, A., Barnes M., and Marjanovic O., Analysis of active power control for VSC HVDC, IEEE Transactions on Power Delivery, vol. 29, no. 4, pp. 1978–1988, 2014.

[24] B. W. Tuinema, E. Adabi, P.K.S. Ayivor, V. Garcia Suarez, L. Liu, A.D. Perilla Guerra, Z. Ahmad, J. L. Rueda Torres, M.A.M.M. van der Meijden, P.Palensky, “ Modelling of Large-sized Electrolysers for Real-Time Simulation and Study of the Possibility of Frequency Support by Electrolysers”, IET Generation, Transmission & Distribution, vol.14, no.10, pp. 1985-1992, 13 May 2020.

[25] P. Ayivor, J. L. Rueda Torres, M.A.M.M. van der Meijden, R. van der Pluijm and B. Stouwie, “ Modelling of Large Size Electrolyzer for Electrical Grid Stability Studies in Real Time Digital Simulation”, in Proc. of Energynautics 3rd International Hybrid Power Systems Workshop, Tenerife, Spain, May 2018.

[26] European Commission, “Commission Regulation (EU) 2017/1485 of 2 August 2017 establishing a guideline on electricity transmission system operation”, European Commission, Brussels 2017.

[27] G.Giannakopoulos, “Master Thesis: Optimal Tuning of the Active Power Gradient Control in Multi-Energy HVDC-HVAC Power Systems”, Delft University of Technonolgy, April 2021, Delft, Netherlands.

978-1-6654-0823-3/22/$31.00 ©2022 IEEE